Hindawi
Journal of Nanomaterials
Volume 2022, Article ID 1165750, 11 pages
https://doi.org/10.1155/2022/1165750

Research Article

Bi-objective Optimization of Process Parameters in Electric Discharge Machining of SS630 Using Grey Relation Analysis

Venkata N. Raju Jampana,[1] **P. S. V. Ramana Rao**,[1] **and Anubhav Kumar**[2]

[1]*Centurion University of Technology and Management, Visakhapatnam, Andhra Pradesh, India*
[2]*School of Computing, Mekelle University, Mekelle, Ethiopia*

Correspondence should be addressed to Venkata N. Raju Jampana; vnrjampana@gmail.com
and Anubhav Kumar; anubhav.kumar@mu.edu.et

Received 6 May 2022; Revised 26 May 2022; Accepted 4 June 2022; Published 23 June 2022

Academic Editor: Samson Jerold Samuel Chelladurai

One of the most former and widely utilized unconventional machining is known as the process of electric discharge machining (EDM). This is a procedure, where a serialized set of electric discharges are applied to eliminate the material from a workpiece (i.e., electrically conductive). This article proposes a bi-objective optimization of process arguments in machining of stainless steel of 630 (SS630) grade using both experimentation and thermal investigation. Here, flushing pressure (P_F), pulse on-time (T_{ON}), peak current (I_p), and pulse off-time (T_{OFF}) are assumed as the input process parameters to conduct a series of experiments on die-sinking EDM (DS-EDM) of SS630 to predict the output characteristics of machining optimization using grey relation analysis (GRA). Both material removal rate (MRR) and surface roughness (SR) are used for evaluating the output response obtained using the machining performance. In addition, thermal investigation is performed using finite element method (FEM) analysis to compute theoretical MRR (T-MRR) for the distribution of temperature on workpiece. Further, GRA is employed to obtain the optimal process parameter combination for best output responses. From the confirmation test results, the optimal combination obtained using GRA approach is at $I_p = 6$A, $T_{ON} = 35\,\mu$s, $T_{OFF} = 90\,\mu$s, and $P_F = 4$ MPa.

1. Introduction

Manufacturing is experiencing many changes because of the frequent demands of the customers for qualitative, reliable, and superior components and merchandises in the most advanced and technological climate. To meet these demands, manufacturers around the globe are working toward cheaper cost solutions to maintain their competitiveness on machined parts and manufactured goods. It is not feasible to procure device products for cutting materials like stainless steel, Nimonics, titanium, satellites, and ceramics. Generation of intricate shapes on such materials is also difficult by traditional techniques. Advanced machining methods have come into existence to match such needs. Such advanced machining methods have unique qualities compared to conventional machining methods. EDM is one of such advanced machining methods, to generate parts with excellence, finesse, and dimensional accuracy [1]. The advanced machining methods are essential as several workpiece materials are actively employed in the automotive enterprises, aerospace part, medical appliances, and molding, and die manufacturing industries. A regulated erosion by a sequence of electric sparks necessitates removing the material in EDM, and the two conductors are immersed in a dielectric medium [2]. For electrical discharge sparking, both conductors are separated by the distance, known as a spark gap. The spark gap is maintained with the help of the servo controller [3]. The transmitted electrons strike with dielectric particles existing in the spark gap so that the plasma channel formed. The plasma channel permits the current to cross the conductors to produce sparks. A significant quantity

of heat produced due to which a few portions of conductors melted and dissipated. After this, the material is melted and vaporized. During the process, several sparks are created, and the workpiece material gets the shape of the electrode. The flushing process can remove the melted material in the air gap [4]. Figure 1 displays the principal schematic picture of the EDM process.

In [5], the authors executed a full scale electrothermal visualization of variable effect on the attributes of solitary spark corrosion used in the procedure of EDM. Additionally, they have also performed theoretical analysis in differentiation with experiment validation. Jithin et al. [6] assumed the equations of Gaussian heat flux and thermal conductivity as temperature relaying properties for finding the experimental radius of carter, which are then compared with predicted carter radius. In [7], the authors performed an improvement on modelling of EDM with the adjoining process of the deformed characteristic of geometry and the thermal study of heat transfer. Due to the proportionality of deformation rate computation with the spark corrosion, the outcome is more accurate and naturalistic result and further validated the simulated outputs by managing examination on AISI OI work steels with the change in the procedure variable of machine such asT_{ON}andI_p. In [8], ANSYS FEM coding is used to calculate the propagation of temperature, and then prediction of volume discarded on account of solitary spark is reckoned from the temperature profiles. Further, T-MRR values are compared with the values of E-MRR. The recent investigation [9] of machining on H13 die steel assumed process variables such as substances of cathodes, anodes, T_{ON}, and I_p for conducting a series of experiments, and the machining process is evaluated using output responses like TWR, MRR, and SR. In addition, Taguchi approach is employed as an optimization of EDM parameters. In [10], MRR is verified on DS-EDM of structural machining of SKD11 die steel with process variables like T_{ON}, I_p, and gap voltage (V_G). Further, the effects of these process parameters also analyzed using response surface methodology (RSM). In [11], the influence of different input process arguments in DS-EDM is experimented and examined with the usage of couple of electrodes such as copper and graphite with both polarities (i.e., positive, and negative) to obtain maximum response of MRR and minimum of SR.

Chekuri et al. [12] studied the DS-EDM on supper alloy made of Nimonic C-263 with graphite electrode using Taguchi L_{25} orthogonal array by considering input process parameters such as I_p, T_{ON}, T_{OFF}, and P_F to obtain the output response characteristics like MRR, TWR, and SR, respectively. Rajamanickam and Prasanna [13] examined the EDM for drilling of small hole on Inconel 718 workpiece with brass electrode (diameter of 300 μm). The authors employed RSM and TOPSIS approaches for describing the significant input process parameters that influence the output response characteristics like MRR, EWR, ovrcut, taper angle and circularity etc. In [14, 15], the authors introduced optimization techniques based on evolutionary algorithms to obtain optimal process parameter combination to reduce the machining time and improving the machining efficiency with enhanced performance. In [16], the concept of artificial intelligence called artificial neural networks

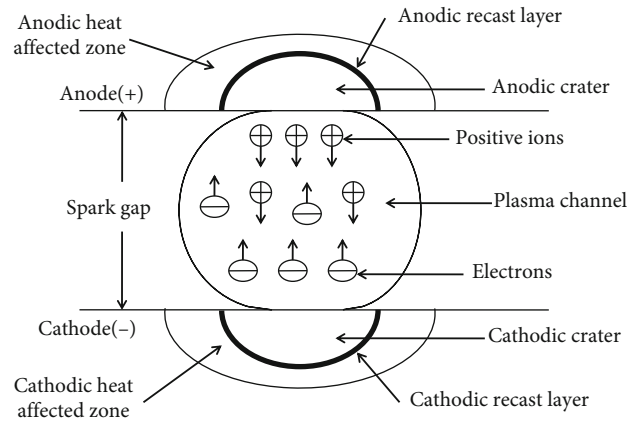

Figure 1: Schematic of EDM process.

is employed to predict the output response parameters such as MRR, SR, and TWR after machining the Nimonic C-263 using DS-EDM process.

Kavimani and Soorya [17] proposed T-GRA-PCA to assess the effect of process variables over the measured machining performance of WEDM performed on magnesium based MMCs. Chaudhari et al. [18] implemented a unique and integrated design for optimizing the control variables such as discharge current, T_{ON}, and T_{OFF} in wire cut EDM process using an approach of GRA. The authors found an optimal combination of input control variables at 6 μsec, 4 μsec, and 6A of T_{ON}, T_{OFF}, and discharge current, respectively. Further, the validation has proven the closest association of optimal outcome as compared to the experimental response. In [19], the authors performed an experimental evaluation with optimization of input control variables in DS-EDM of AISI D2 steel, where the optimal combination is obtained using integrated RSM with GRA technique. The obtained optimal combination of process variables such as discharge current, gap of spark, dielectric liquid, and electrode polarity are 15A, 6 mm, kerosene oil, and positive polarity, respectively. The confirmation test results have been verified and validated the enhancement in machining process. Mitra et al. [20] performed an induration process by creating a highly nonlinear model with twenty-two dimensional principles and implemented an architecture of neural network with multilayer perceptron for solving an optimization issue with multiple objectives. In [21], the authors experimented and validated the impact of various control variables such as V_G, T_{ON}, and I_p on DS-EDM of SS with grade AISI420 material. They have measured MRR and electrode wear rate as output response attributed for performance validation. Additionally, the integrated Taguchi with GRA is applied to find the best possible combination for optimal machining on DS-EDM. Jampana and Ramana Rao [22] investigated an experimental analysis of DS-EDM on SS630 grade with machining control variable optimization using a design approach of Taguchi for an output response attributes such as MRR, and SR. However, the machining parameter optimization is still a challenging job for improving the productivity and reducing the labor time which influences the overall production cost in the applications of manufacturing filed. In

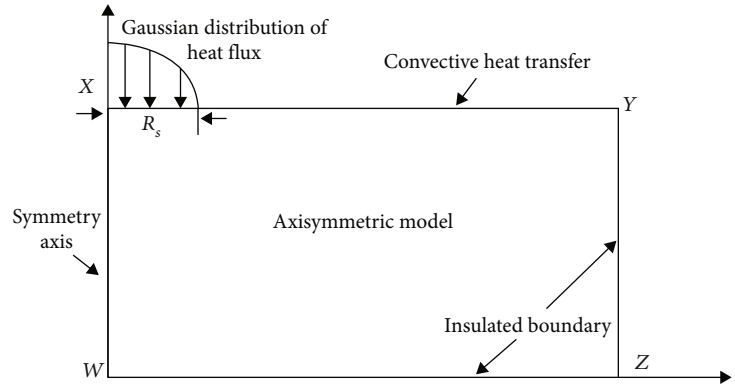

Figure 2: 2D symmetric axis sharing its partition with DS-EDM process.

Table 1: Workpiece material compositions with corresponding weight.

Name of component	% of weight
Silicon (Si)	0.40 max
Nickel (Ni)	10.00-14.00
Manganese (Mn)	0.60-1.00 max
Carbon (C)	0.036-0.44 max
Chromium (Cr)	16.00-18.00
Sulphur (S)	0.030 max
Nitrogen (N)	0.10 max
Phosphorus (P)	0.05 max
Molybdenum (Mo)	2.00-3.00
Iron (Fe)	Balance

Table 2: Fundamental attributes of composition of electrode material.

Name of composition	Density ($g/cm^3 \geq$)	Hardness (Kgf/mm^2)	Resistivity ($\mu\Omega cm$)
*W*50/*Cu*50	11.849	114.99	3.199

substance, the main problems arisen in DS-EDM process are due to the generation of heat. Therefore, addressing the temperature alterations in workpiece material is essential to enhance the performance before starting the machining process, which can be achieved using thermal investigation techniques like FEM analysis [23, 24]. Recently, Chekuri et al. [25] studied the experimental and numerical investigation of DS-EDM on Nimonic C-263 as workpiece material with an electrode tool of copper-tungsten. In addition, hybrid optimization approach called the cuckoo search-based whale optimization algorithm is implemented for obtaining the optimal combination of machining control variables for increased performance. However, none of the works addressed in the literature have not examined FEM analysis of DS-EDM on SS630 grade. In addition, it is quite sturdy to do machining of a workpiece made of SS630 grade material because of its properties such as lesser thermal conductivity, higher erosive resistance, and higher built-up edge tendency. Further, this product has a variety of applications in industries such as pharmaceutical, pumping production, and other device paradigms.

Table 3: Input control variables with their corresponding levels.

Parameter	No. of levels			
	Level 1	Level 2	Level 3	Level 4
I_p (A)	6	10	14	18
T_{ON} (μs)	15	25	35	45
T_{OFF} (μs)	20	50	70	90
P_F (Mpa)	2	4	6	8

Hence, this article addresses a thermal and experimental evaluation of DS-EDM on a workpiece made of using SS630 grade material with an electrode tool of copper-tungsten. Initially, the temperature distribution profiles are observed using the FEM analysis, and T-MRR is computed using an isotherm of temperature. Additionally, GRA technique is employed as a solution for solving the optimization problem, which predicts the optimal combination of machining control variables.

2. Prerequisite for FEM Analysis

This paragraph states the various inspection of DS-EDM procedure utilizing the scanning of the FEM, which is preferred for replicating single spark with the EDM by obtaining numerous properties such as variable spark radius, cathode energy fraction, and evenly distributing the equation for Gaussian heat flux. The following are the considerations for numerical analysis:

(i) Workpiece substance is homogeneous and isotropic

(ii) Vitality fragment is depending on T_{ON}

(iii) 297 K: required temperature

(iv) Modeling for solitary spark

(v) 100%: effective flushing

The equation properties of Fourier heat condition are employed to derive the governing equation that operates FEM.

Table 4: Working circumstances for setting up the experimentation.

Name	Description
Workpiece material	SS630 grade $(70 \times 40 \times 8mm)$
Electrode material	Copper-tungsten (21.5 mm length with a diameter of 12.5 mm)
Dielectric oil	Commercial EDM oil grade SAE 450
Sign of polarity	Normal
Supply voltage	110 V
Gap voltage	70 V
Time of machining	5 mins

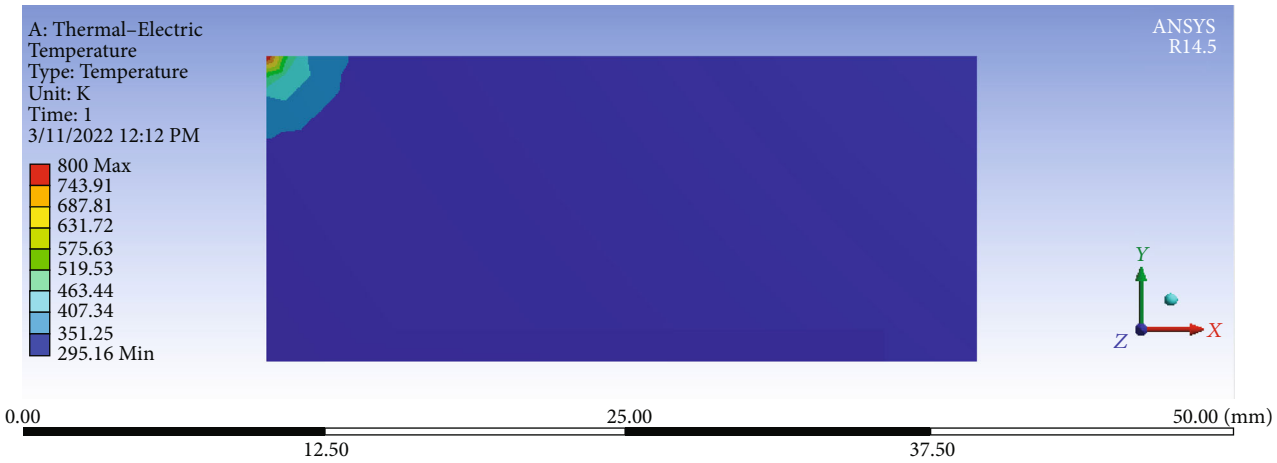

Figure 3: Distribution of temperature distribution attained for 18A of current intensity and 45 μsec of pulse duration.

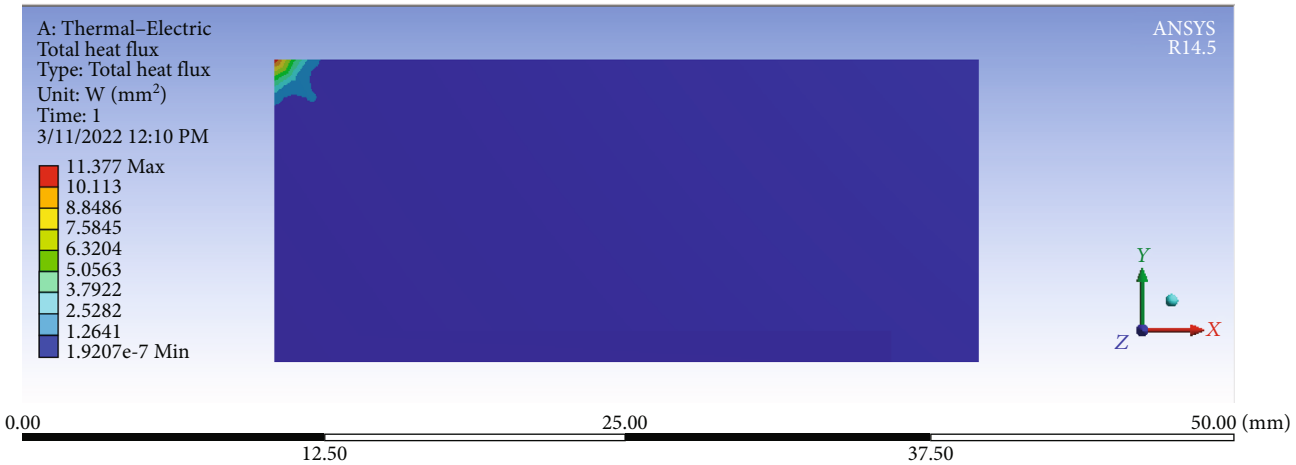

Figure 4: Amount of material removed for 18A of current intensity and 45 μsec of pulse duration.

2.1. Governing Equation. The differential equations stated below are employed to manage the conduction of thermal generated heat in axisymmetric model:

$$\rho C_p \frac{\partial T}{\partial t} = \frac{1}{r}\frac{\partial}{\partial r}\left(K_t r \frac{\partial T}{\partial r}\right) + \frac{\partial}{\partial z}\left(K_t \frac{\partial T}{\partial z}\right). \quad (1)$$

C_p is denoted as specific heat, ρ is workpiece, T is temperature, and K_t is thermal conductivity. The r and z are denoted by cylindrical workpiece.

2.2. Boundary Conditions. Figure 2 represents the 2D axisymmetric model which is introduced with frontier conditions that is on the north side of XY surface. The properties of

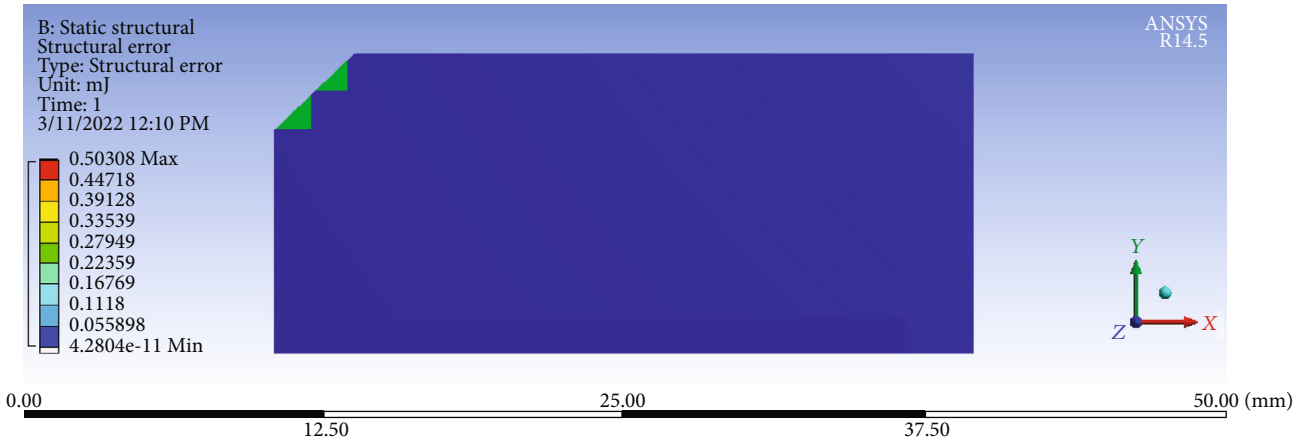

Figure 5: Structural error.

Figure 6: Machining procedure of DS-EDM.

Figure 7: Illustration of SS630 grade workpiece after machining.

nature Gaussian distribution are utilized by spark radius aimed overall with the ignition on heat flux time. Heat transfer beyond the spark radius is the convective generation of cooling effect of dielectric. Here, the value of heat flux is considered as negligible almost zero. XW is denoted as axisymmetric boundary, and WZ and YZ are two other boundaries, which are far from the radius of spark, severally.

2.3. Heat Input. In general, DS-EDM has some significant factors such as workpiece heat input and the measure of thermophysical properties, where the preference of these parameters impacts the estimation of MRR values. The approximation of generated heat from plasma of transitory model is done using Gaussian heat distribution as formulated below:

$$q_w(r) = \frac{4.45PV_GI_p}{\pi R_s^2} \exp\left\{-4.5\left(\frac{r}{R_s}\right)^2\right\}, \quad (2)$$

where V_G is denoted as the gap voltage, R_s is represented as spark radius, I_p is denoted as peak current, P is denoted as amount of temperature gained by the workpiece, and q_w is represented as the temperature quantity in the workpiece through the sparking operation.

2.4. Spark Radius. In real-time cases, it is a tough task to calculate short pulse duration with the spark radius. Thus, for calculation of this spark radius constructively, numerous methods had been listed in the literature. In those, Erden23 has shown that the discharge power and time are directly proportional to spark radius, which is expressed as follows:

$$R_s = ZP^mT_{on}^n, \quad (3)$$

where m, n, and Z are represented as empirical constants; T_{on} denotes pulse on-time; and P and R_s represent the power and spark radius, respectively.

2.5. Solution Methodology for Thermal Analysis. With the implementation of FEM, control equation specified in Equation (1) can be resolved by acquiring the ANSYS 15.0 visualization domain. The size of the workpiece for thermal analysis is

Table 5: Obtained experimental values of MRR, and SR for the input process variables.

Experiment no.	I_p (A)	T_{ON} (μs)	P_F (MPa)	T_{OFF} (μs)	E-MRR (mm^3/min)	SR (μm)
1	6	15	2	20	1.372	3.29
2	10	15	4	50	5.015	3.92
3	14	15	6	70	2.412	4.12
4	18	15	8	90	3.421	4.45
5	14	25	4	20	5.522	4.56
6	18	25	2	50	6.101	5.12
7	6	25	8	70	2.585	3.12
8	10	25	6	90	3.921	4.21
9	18	35	6	20	3.812	5.31
10	14	35	8	50	4.912	4.92
11	10	35	2	70	8.156	4.72
12	6	35	4	90	9.121	3.56
13	10	45	8	20	4.125	4.31
14	6	45	6	50	3.912	3.84
15	18	45	4	70	10.121	5.54
16	14	45	2	90	9.312	5.62

Table 6: Grey relation generation values for output response parameters obtained using DS-EDM of SS630 with Cu-W electrode.

Ideal seq.	MRR (mm^3/min) Larger the better	SR (μm) Smaller the better
1	0	0.932
2	0.41639	0.68
3	0.118871	0.6
4	0.234198	0.468
5	0.47434	0.424
6	0.540519	0.2
7	0.138644	1
8	0.291348	0.564
9	0.278889	0.124
10	0.404618	0.28
11	0.775403	0.36
12	0.885701	0.824
13	0.314665	0.524
14	0.290319	0.712
15	1	0.032
16	0.907532	0

assumed as $15 \times 10 \times 3$ mm, where element size is assumed as 1 μm and then the model mesh and dimensions are created. FEM is an application to gain the organizing of the heat quotient on the workpiece, and the values of MRR are calculated from the workpiece as shown below:

$$MRR = \frac{C_v \times 60}{T_{ON} + T_{OFF}(\text{sec})}, \quad (4)$$

where C_v is denoted crater volume and T_{ON} and T_{OFF} are represented as pulse on-time and pulse off-time.

3. Materials and Methods

Here, SS630 grade material is selected as a workpiece due to low risk of distortion at reduced temperatures. It has 8 mm thickness and 70×40 mm rectangular dimensions. Additionally, it is a best choice for an experimentation on DS-EDM when there is a necessity of erosion and higher strength. The electrode material used in this work is a copper-tungsten mixture since they are not mutually solvable.

The electrode length is about 21.5 mm and 12.5 mm diameter. The chemical composition of workpiece material and the properties of electrode material are listed in Tables 1 and 2, respectively.

4. Experimental Setup

This section contains numerous process variables with all ideal levels and experimental setup. All the experimental trials are performed using FORMATICS 50 on an apparatus of DS-EDM model, which is embedded with ELECTONICA PRS 20 to analyze the effects of various elements of process variables such as T_{OFF}, T_{ON}, P_F, and I_p on the SR of machine drilled hole. In addition, MRR also computed during the process of DS-EDM of SS 630 grade with copper-tungsten electrode. Before starting themachining process of DS-EDM , the experimentation tools like electrode, and workpiece are well polished and cleaned. The control variables of input to the DS-EDM are listed in Table 3 with their number of levels, while the working conditions and their explanation for setting up the experimentation is listed in Table 4, respectively. Additionally, the SR is measured on machined surfaces with the direction of transverse on machine surface of cutoff length as 0.8 mm using Talysurf SR tester. The final values of SR are measured using the iterative mechanism, where it was tested thrice and considered the averaged value as final SR.

4.1. Thermal Investigation Using FEM. In practice, the commercial FE code is integrated in DS-EDM process to estimate the distribution of temperature and the deformation of molten material using the plasma pressure. On the other hand, FE code is employed by ANSYS for verifying the solutions for real-time problems. The complicated interlinkage of numerous material phenomenon is intricated in DS-EDM which is again a complex thermal process. Therefore, FEM analysis is applied to simulate the distribution of temperature and stress analysis into the workpiece; here, an advanced software, i.e., ANSYS, is utilized for upgrading the DS-EDM model with FEM analysis for all complex parameters processing. This can be utilized with various models and determine any complex geometry which consists various capacities of FEM varying from thermal system, and fluid mechanics, simple linear structure to static analysis of nonlinear complex structures, structural mechanics, varying dynamic survey, and electromagnetics.

This work considered ANSYS 14.5 workbench for simulating the results on modelling of DS-EDM with SS630 grade

Table 7: Obtained GRC and GRG values with their corresponding ranks.

Ideal Seq.	Deviation seq.		GRC		GRG	Rank
	MRR (mm^3/min)	SR (μm)	MRR (mm^3/min)	SR (μm)		
1	1	0.068	0.333333	0.880282	0.606808	4
2	0.58361	0.32	0.461421	0.609756	0.535588	7
3	0.881129	0.4	0.362023	0.555556	0.458789	12
4	0.765802	0.532	0.395007	0.484496	0.439751	14
5	0.52566	0.576	0.487491	0.464684	0.476087	9
6	0.459481	0.8	0.521115	0.384615	0.452865	13
7	0.861356	0	0.367281	1	0.68364	2
8	0.708652	0.436	0.413684	0.534188	0.473936	10
9	0.721111	0.876	0.409463	0.363372	0.386418	16
10	0.595382	0.72	0.456462	0.409836	0.433149	15
11	0.224597	0.64	0.690039	0.438596	0.564318	6
12	0.114299	0.176	0.813936	0.739645	0.776791	1
13	0.685335	0.476	0.421822	0.512295	0.467058	11
14	0.709681	0.288	0.413332	0.634518	0.523925	8
15	0	0.968	1	0.340599	0.6703	3
16	0.092468	1	0.843928	0.333333	0.588631	5

Table 8: Response table for mean GRG.

Level	T_{ON}	T_{OFF}	P_F	I_p
1	0.5102	0.4841	0.5532	0.6478
2	0.5216	0.4864	0.6147	0.5102
3	0.5402	0.5943	0.4608	0.4892
4	0.5625	0.5698	0.5059	0.4873
Delta	0.0522	0.1102	0.1539	0.1605
Rank	4	3	2	1

Table 9: Response table for signal to noise ratios (larger is better).

Level	T_{ON}	T_{OFF}	P_F	I_p
1	-5.916	-6.414	-5.198	-3.863
2	-5.779	-6.296	-4.385	-5.873
3	-5.672	-4.629	-6.782	-6.271
4	-5.076	-5.105	-6.080	-6.437
Delta	0.840	1.785	2.397	2.575
Rank	4	3	2	1

with the development of geometrical work via precise constraints of boundary and employing variable loads. An approach called mapped meshing is utilized for meshing the domain of workpiece. As it is shown in Figures 3–5, there are four different regions with distinct colors such as red, light green, light blue, and blue, whereas the red and blue colors denote the region of boiling and solid metal, while the light green and light blue denote the zones of liquid and heat affected, respectively. Usually, the distribution of temperature on workpiece relies on input control variables such as input heat percentage, T_{ON}, I_p, T_{OFF}, and V_G along with the change in phase. Figure 3 demonstrates the distribution of temperature attained for 18A of current intensity with 45 μsec of pulse duration, where the maximum and minimum distributed temperatures are about 800 K and 295.16 K. Figure 4 illustrates the amount of material removed for the same current intensity with pulse duration, where the maximum and minimum heat flux is about 11.337 w/mm^2 and 1.26 w/mm^2. The structural error is demonstrated in Figure 5.

4.2. Results. Figure 6 illustrates the processing of machining with DS-EDM on SS630 grade, while Figure 7 demonstrates the workpiece after machining of SS630. As mentioned earlier, MRR and SR are used as he output response parameters for evaluating the performance of DS-EDM on SS630 grade. Table 5 lists with the obtained results of output response parameters with varying of input control parameters.

5. Optimization Using GRA

In a problem of multiresponse, the influence and relationship between different parameters are complex and not clear. This is termed as grey which signifies poor and uncertain information. The proposed GRA analyzes this complicated uncertainty among the multiresponses in each system and optimizes it with the help of grey relational grade (GRG). Therefore, a multiresponse optimization problem is reduced to a single response optimization problem called single relational grade. The detailed procedure of GRA is described as below:

Step 1: The first step of GRA involves in the normalization of output response parameters such as MRR and SR for avoiding distinct units and variability mitigation. This is essential due to that differentiation in one data varies from another data. An actual value is utilized to gain an appropriate value which makes the array in the range of [0, 1]. Usually, this is an approach of transforming the actual data into a corresponding

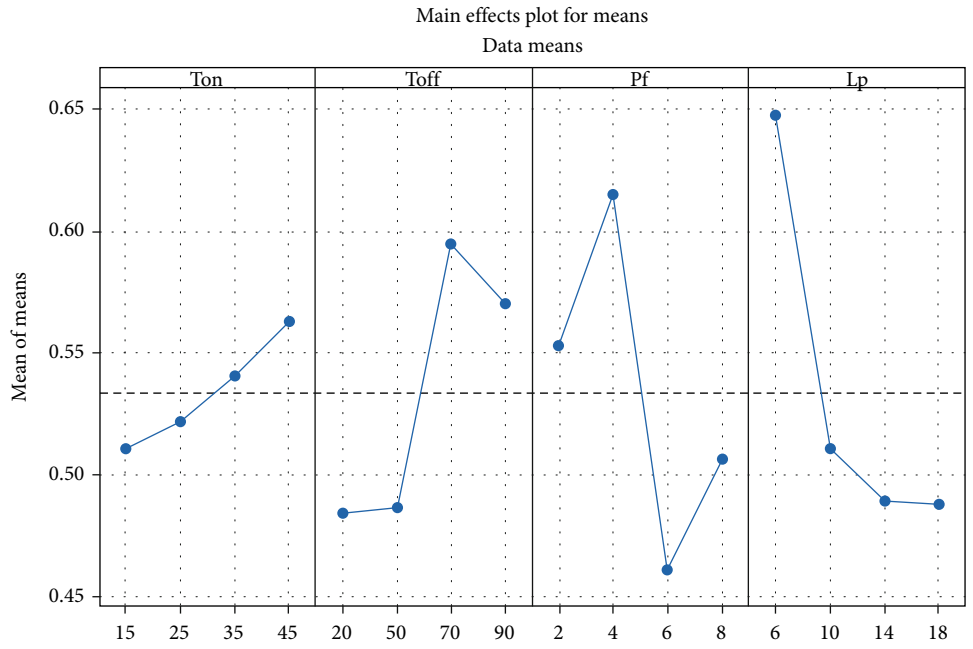

Figure 8: Main effect plot of mean GRG.

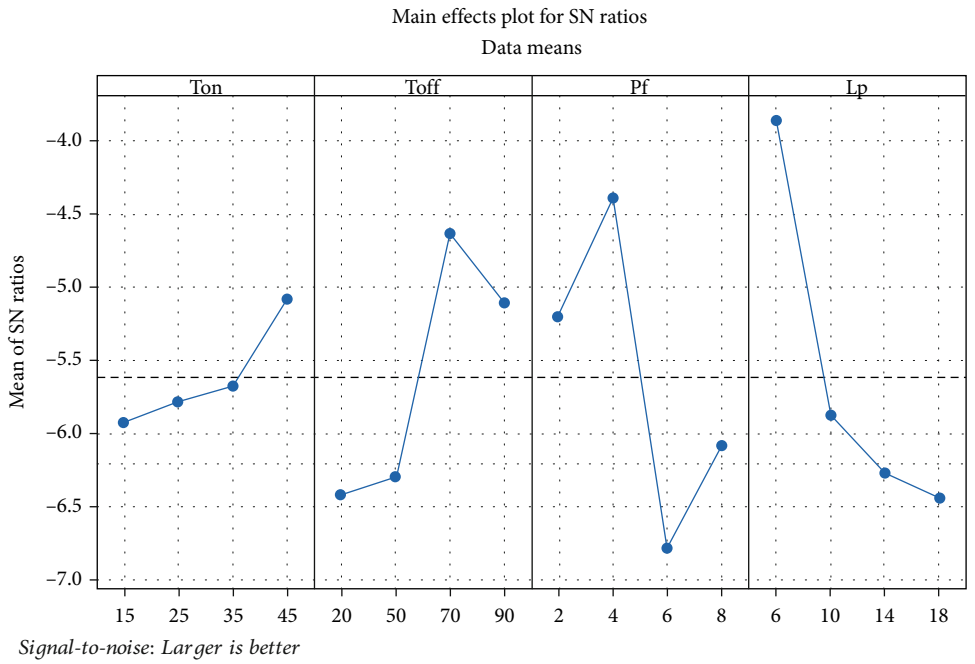

Figure 9: Main effect plot of mean of S/N ratios.

data. If the required observation is to be minimized, the smaller-the-better attributes are proposed for the normalization to surmount it into a satisfactory range using the below formulation:

$$x^*_i(k) = \frac{\max x_i(k) - x_i(k)}{\max x_i(k) - \min x_i(k)}, i = 1, \cdots, m; k = 1, \cdots, n, \quad (5)$$

where the desired value is denoted with x. The data quantity of experiments and the corresponding response are referred to m and n. The actual and preprocessed sequence are denoted as $x_i(k)$, and $x^*_i(k)$, respectively. The maximum and minimum values of actual data are represented as max $x_i(k)$, and min $x_i(k)$. Table 6 demonstrates the grey relation generation values for output attributes named MRR and SR where maximum is better and minimum is better, respectively.

Table 10: Obtained results of ANOVA on GRG of DS-EDM on SS630.

Source	DF	Adj. SS	Adj. MS	F value	P value	Remarks
T_{ON}	3	0.006265	0.002088	1.07	0.479	"Insignificant"
T_{OFF}	3	0.038677	0.012892	6.59	**0.078**	"Significant"
P_F	3	0.052121	0.017374	8.87	**0.053**	"Significant"
I_p	3	0.070804	0.023601	12.06	**0.035**	"Significant"
Error	3	0.005873	0.001958			
Total	15	0.173740				

Table 11: Obtained values of T-MRR and E-MRR with machining control variables.

S. No.	I_p (A)	P_F (MPa)	T_{OFF} (μs)	T_{ON} (μs)	E-MRR (mm^3/min)	T-MRR (mm^3/min)
1	6	2	20	15	1.372	1.512
2	10	4	50	15	5.015	4.912
3	14	6	70	15	2.412	2.321
4	18	8	90	15	3.421	3.614
5	14	4	20	25	5.522	5.23
6	18	2	50	25	6.101	5.90
7	6	8	70	25	2.585	2.421
8	10	6	90	25	3.921	3.672
9	18	6	20	35	3.812	3.612
10	14	8	50	35	4.912	5.21
11	10	2	70	35	8.156	8.912
12	6	4	90	35	9.121	9.461
13	10	8	20	45	4.125	3.671
14	6	6	50	45	3.912	3.876
15	18	4	70	45	10.121	11.24
16	14	2	90	45	9.312	8.91

Step 2: The second step is to compute the grey relation coefficient (GRC) denoted as $\xi_i(k)$ from the obtained normalized values in Step 1. The computation of GRC is as follows:

$$\xi_i(k) = \frac{\Delta_{\min} + \xi\Delta_{\max}}{\Delta_{0i}(k) + \xi\Delta_{\max}}, \tag{6}$$

where $\Delta_{0i}(k)$ denotes the deviation sequence of the reference sequence and $\Delta_{0i} = \|x_0(k) - x_i(k)\|$ represents the sequence of comparability, where the reference and comparability sequences are termed as $x_0(k)$, and $x_i(k)$, respectively.

The larger and smaller values of absolute differences of all the comparability sequences are represented as $\Delta_{\min}$ and $\Delta_{\max}$. The coefficient of identification is denoted as ξ with the range of $[0, 1]$. In general, this value will be considered as 0.5.

Step 3: This step computes the grey relation grade (GRG) as shown below:

$$\gamma_i = \frac{1}{n}\sum_{k=1}^{n} \xi_i(k), \tag{7}$$

where the required GRG is represented as γ_i for i^{th} experiment and n denotes the response attributes quantity. In general, this GRG determines the level of association between the sequences of reference and comparability. On the other side, it also represents the overall illustration of all the quality attributes. Therefore, the optimization problem of multiple responses can be transformed into a solitary optimization issue using the design approach of Taguchi with integration of GRA technique. Table 7 lists the obtained GRC and GRG with ranking values for the bi-objective optimization of MRR and SR responses.

Step 4: Now, this stage determines the control variables optimal level using the maximum GRG which designates an improved quality of product. To get this, the aggregated grade values of all machining control variables should be derived as listed in Table 8, which is called a table of mean responses where the maximum of average grade values are selected as an optimal machining control variable combination for multiple responses.

Table 9 illustrates the response table for signal to noise (S/N) ratios. Figures 8 and 9 disclose the main effect plots of GRG and S/N ratios, respectively.

Step 5: This stage uses analysis of variance (ANOVA) to determine the relevant factors influencing the different responses with the confidence level of 90%, which provides valuable data about experimental requirements. So, the process of ANOVA avoids the unwanted experimentations by selecting the best combination of EDM performance properties. Further, the ANOVA analysis will be useful in determining the contribution percentage to recognize parameter dependent effects generated from EDM, because the influence of each parameter on multiple response cannot be measured using Taguchi's design technique. The ANOVA divides the entire variability of the answer such as squared sum deviations generated from grand mean with the error and parameter contributions. Here, probability of significance is considered as P values, and it is calculated using Fisher's F ratio (F value), which tells the importance of each processing parameter. Further, the range of P values should be less than 0.1, which indicates the significant parameters. If the P value (probability of significance) is less than 0.1, the P value is determined based on the F value or to get information about the importance of the chosen answer. In addition, the mean square (MS) is generated by dividing the degrees of freedom (DF) with available independent data-based sum of squares (SS), i.e., MS = SS/DF. Moreover, in the optimal parameters obtained scenario, F value is equivalent to MS, i.e., F = MS. Table 10 shows the GRG based ANOVA simulation findings with the importance of process parameters on multiple responses.

Step 6: This step enhances the GRG by investigating confirmation test results. Finally, the GRG predicted values for optimal level can be obtained as follows:

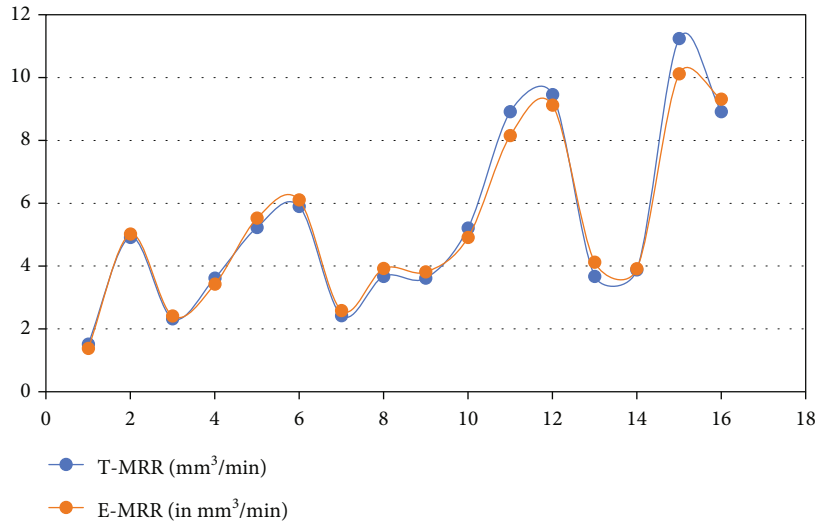

Figure 10: Comparison of E-MRR and T-MRR obtained using FEM analysis and experimentation of DS-EDM on SS630.

$$\widehat{\gamma} = \gamma_m + \sum_{i=1}^{o} (\bar{\gamma}_i - \gamma_m), \tag{8}$$

where the total mean GRG is denoted with γ_m, the mean GRG at the optimal level of each parameter is represented as γ_i, and o is the number of the significant process parameters. Table 11 lists the obtained values of T-MRR, and E-MRR with machining control variables for L_{16} orthogonal array. The validation of DS-EDM on SS630 grade is done using the obtained T-MRR computed from isotherm of temperature observed from FEM analysis with the values of E-MRR obtained from experimental analysis. Figure 10 illustrates the comparative analysis of E-MRR and T-MRR which discloses a very close relation between numerical and experimental values of MRR.

6. Conclusion

This article aimed on experimental and thermal investigation of DS-EDM with bi-objective optimization using GRA approach. In addition, FEM analysis also employed to compute the T-MRR using 2-D axisymmetric with its boundary conditions by distributing the Gaussian flux. Further, GRA is used and found the best fit and approximate solutions for obtaining the optimal combination of process parameters such as I_p, T_{ON}, T_{OFF}, and P_F. From the confirmation test results, the optimal combination obtained using GRA approach is about 12^{th} experiment, i.e., $I_p = 6$A, $T_{ON} = 35\,\mu$s, $T_{OFF} = 90\,\mu$s, and $P_F = 4$ MPa. The most significant process parameters identified using ANOVA are I_p, P_F, and T_{OFF} with 90% confidence values.

Data Availability

The data used to support the findings of this study are included within the article.

Disclosure

This study was performed as a part of the Employment of Mekelle University, Tigray, Ethiopia.

Conflicts of Interest

Authors declared that there is no conflict of interest in publication.

References

[1] R. K. Shastri, C. P. Mohanty, S. Dash, K. M. P. Gopal, A. R. Annamalai, and C.-P. Jen, "Reviewing performance measures of the die-sinking electrical discharge machining process: challenges and future scopes," *Nanomaterials*, vol. 12, no. 3, p. 384, 2022.

[2] K. H. Ho and S. T. Newman, "State of the art electrical discharge machining," *International Journal of Machine Tools and Manufacture*, vol. 43, no. 13, pp. 1287–1300, 2003.

[3] T. Muthuramalingam and B. Mohan, "Influence of discharge current pulse on machinability in electrical discharge machining," *Materials and Manufacturing Processes*, vol. 28, no. 4, pp. 375–380, 2013.

[4] M. P. Groover, *Fundamentals of Modern Manufacturing: Materials, Processes, and Systems*, Wiley, Danvers, 4th edition, 2010.

[5] A. Ahmed, A. Fardin, M. Tanjilul, Y. S. Wong, M. Rahman, and A. S. Kumar, "A comparative study on the modelling of EDM and hybrid electrical discharge and arc machining considering latent heat and temperature-dependent properties of Inconel 718," *The International Journal of Advanced Manufacturing Technology*, vol. 94, no. 5-8, pp. 2729–2737, 2018.

[6] S. Jithin, A. Raut, U. V. Bhandarkar, and S. S. Joshi, "FE modeling for single spark in EDM considering plasma flushing efficiency," *Procedia Manufacturing*, vol. 26, pp. 617–628, 2018.

[7] E. L. Papazoglou, A. P. Markopoulos, S. Papaefthymiou, and D. E. Manolakos, "Electrical discharge machining modeling by coupling thermal analysis with deformed geometry

feature," *The International Journal of Advanced Manufacturing Technology*, vol. 103, no. 9-12, pp. 4481–4493, 2019.

[8] R. Rajendran and S. P. Vendan, "Single discharge finite element simulation of EDM process," *Journal of Advanced Manufacturing Systems*, vol. 14, no. 2, pp. 75–89, 2015.

[9] M. M. Bahgat, A. Y. Shash, M. Abd-Rabou, and I. S. El-Mahallawi, "Influence of process parameters in electrical discharge machining on H13 die steel," *Heliyon*, vol. 5, no. 6, pp. e01813–e01813, 2019.

[10] N. H. Phan, N. V. Duc, and P. V. Bong, "Application of response surface methodology for evaluating material removal rate in die sinking EDM roughing using copper electrode," *Science and Technology Development Journal-Engineering and Technology*, vol. 1, no. 1, pp. 20–27, 2018.

[11] M. M. Bahgat, A. Y. Shash, M. Abd-Rabou, and I. S. El-Mahallawi, "Effects of process parameters on the machining process in die-sinking EDM of alloyed tool steel," in *Engineering Design Applications III.*, H. A. AÖ, Ed., vol. 124, Springer, 2020.

[12] R. B. R. Chekuri, R. Kalluri, J. K. Palakollu, and R. Siriyala, "Modeling and optimization of machining high performance nickel based super alloy nimonic C-263 using die sinking EDM," *International Journal of Mechanical Engineering and Robotics Research*, vol. 8, no. 2, pp. 196–201, 2019.

[13] S. Rajamanickam and J. Prasanna, "Application of TOPSIS to Optimize EDM Process Parameters for Small Hole Drilling of Inconel 718," in *Advances in Manufacturing Processes*, K. Vs and A. A. Mg, Eds., Springer, 2019.

[14] N. Faisal and K. Kumar, "Optimization of machine process parameters in EDM for EN 31 using evolutionary optimization techniques," *Technologies*, vol. 6, no. 2, pp. 54–54, 2018.

[15] D. G. Dilip, S. Panda, and J. Mathew, "Characterization and parametric optimization of micro-hole surfaces in micro-EDM drilling on Inconel 718 superalloy using genetic algorithm," *Arabian Journal for Science and Engineering*, vol. 45, no. 7, pp. 5057–5074, 2020.

[16] R. B. R. Chekuri, R. Kalluri, R. Siriyala, and J. K. Palakollu, "A study on die sinking EDM of nimonic C-263 super alloy: an intelligent approach to predict the process parameters using ANN. International journal of," *Engineering and Technology*, vol. 7, no. 1.1, pp. 651–654, 2017.

[17] V. Kavimani, K. S. Prakash, T. Thankachan, S. Nagaraja, A. K. Jeevanantham, and J. P. Jhon, "WEDM parameter optimization for silicon@r-GO/magnesium composite using Taguchi based GRA coupled PCA," *SILICON*, vol. 12, no. 5, pp. 1161–1175, 2020.

[18] R. Chaudhari, J. Vora, D. M. Parikh, V. Wankhede, and S. Khanna, "Multi-response optimization of WEDM parameters using an integrated approach of RSM–GRA analysis for pure titanium," *Journal of the Institution of Engineers (India): Series D*, vol. 101, no. 1, pp. 117–126, 2020.

[19] M. Hanif, W. Ahmad, S. Hussain, M. Jahanzaib, and A. Shah, "Investigating the effects of electric discharge machining parameters on material removal rate and surface roughness on AISI D2 steel using RSM-GRA integrated approach," *International Journal of Advanced Manufacturing Technology*, vol. 101, no. 5-8, pp. 1255–1265, 2019.

[20] S. S. Miriyala and K. Mitra, "Multi-objective optimization of iron ore induration process using optimal neural networks," *Materials and Manufacturing Processes*, vol. 35, no. 5, pp. 537–544, 2020.

[21] S. Kumar, S. K. Ghoshal, P. K. Arora, and L. Nagdeve, "Multivariable optimization in die-sinking EDM process of AISI420 stainless steel," *Materials and Manufacturing Processes*, 2021.

[22] V. N. R. Jampana and P. S. V. Ramana Rao, "Experimental investigation and optimization of die-sinking EDM of grade 630 stainless steel using Taguchi approach," *Materials Today Proceedings*, vol. 36, no. 5, pp. 572–582, 2021.

[23] M. Quarto, G. D'Urso, C. Giardini, G. Maccarini, and M. Carminati, "A comparison between finite element model (fem) simulation and an integrated artificial neural network (ANN)-particle swarm optimization (PSO) approach to forecast performances of micro electro discharge machining (micro-EDM) drilling," *Micromachines*, vol. 12, no. 6, p. 667, 2021.

[24] V. N. R. Jampana, P. S. V. Ramana Rao, and A. Sampathkuamr, "Experimental and thermal investigation on powder mixed EDM using FEM and artificial neural networks," *Advances in Materials Science and Engineering*, vol. 2021, Article ID 8138294, 12 pages, 2021.

[25] R. B. R. Chekuri, D. Eshwar, T. K. Kotteda, and R. S. Srikanth Varma, "Experimental and thermal investigation on die-sinking EDM using FEM and multi-objective optimization using WOA-CS," *Sustainable Energy Technologies and Assessments*, vol. 50, article 101860, 2022.